

# Combined MRI-rheometry determination of the behavior of mud suspensions

P. Coussot & J. S. Raynaud

*LMSGC (UMR 113 LCPC-ENPC-CNRS), France*

C. Ancey

*Cemagref, France*

*Keywords:* rheology, natural mud, magnetic resonance imaging, Herschel-Bulkley equation

**ABSTRACT:** Combining magnetic resonance imaging (MRI) and rheometry is a powerful method for deducing the constitutive equation of a fluid. Using this technique, we have carried out experiments on different types of fine mud suspensions. In steady state, the flow profile within coaxial cylinders is systematically composed of two regions: within the first one, the material is sheared at a rate larger than a critical, finite value ( $\dot{\gamma}_c$ ); in the second one, the material remains unsheared on average. This means that mud flows are basically unstable: they tend to stop flowing abruptly when the imposed stress reaches a critical value (associated with  $\dot{\gamma}_c$ ). This contrasts with the behavior of an ideal yield stress fluid, predicting that the shear rate continuously tends to zero as the difference between the imposed stress and the yield stress tends towards zero. A rheological analysis of the flow profiles demonstrates that the behavior of the sheared region can be very accurately represented by a simple power-law model. These results show that, at low velocities, mudflows are mainly governed by a concentration of the strain in the regions of higher stresses.

## 1 INTRODUCTION

Natural flows of mud suspensions (broadly speaking, including a wide range of phenomena: mudflow, lahar, etc.) are a major natural hazard. A better understanding of their flow characteristics requires a relevant determination of the constitutive equation of the material involved. Natural mud suspensions have the common characteristic of a high concentration of solid particles dispersed in water. Here we will focus on the rheological behavior of suspensions basically composed of sufficiently small (in general colloidal) particles so that (i) the migration of the liquid through the solid matrix *a priori* remains negligible for a typical flow duration (one-phase flow approximation holding for the bulk) (ii) bulk behavior of mud samples depends mainly on the interstitial fluid.

In most cases, these materials are (non-Newtonian) yield stress fluids, i.e., they can flow only when a critical stress is overcome. Simple models used for representing this behavior are the *Bingham model* and the *Herschel-Bulkley model*, which is more accurate. Various experimental data, mainly in rheometry, but also from free surface channelized flows, tend to prove the validity of such a representation of the behavior (Johnson 1970, O'Brien & Julien 1988, Major & Pierson 1992, Coussot 1994, Johnson & Martosudarmo 1997, Contreras & Davies 2000). Some of these fluids have also been shown to be *thixotropic*, i.e., their viscosity changes over time, but this property remains relatively hard to model properly, in particular because of a lack of complete data.

Yield stress as a true property of suspensions is a notion which is both poorly understood and often controversial. In the last 20 years, many methods have been developed for measuring yield stress [see, for instance, the review paper by Nguyen & Boger (1992)]. However, it is not unusual to find that significantly different yield stress values can be obtained using different techniques or different

procedures for a given suspension as exemplified by Alderman et al. (1991) . This in particular has led to the distinction between *dynamic yield stress*, i.e., the stress limit for an infinitely low shear rate, and *static yield stresses*, which are observed after different rest times (Cheng 1986). Moreover “flow curves with a minimum” have been reported for clay-water mixtures (bentonite, laponite) and alumina suspensions: the authors observed fracturing below a critical shear rate (Coussot et al. 1993) or a decrease in stress at low shear rates in steady state (leading to the minimum in flow curve) (Pignon et al. 1996). In the latter case, Pignon et al. (1996) demonstrated with a transparent suspension that, as the shear rate decreases below a critical value, the deformation is localized in a thinner region. Recently, it was suggested that this peculiar behavior is general for concentrated colloidal suspensions and results from the yielding and thixotropic characteristics of the fluid, two effects which appear intimately related (Coussot et al. 2002).

It is usually observed that natural mud, resulting from the mixing of a wide range of clays, ions, and noncolloidal particles exhibits rheological properties that are less pronounced than those of pure concentrated colloidal dispersions. Thus it is not clear whether the flow features described above are representative of natural muds. If so, a second question arises: how do these new results modify the current knowledge of mudflow rheology, knowledge which has so far been mainly built on conventional rheometrical experiments? The purpose of the present study was to review the behavior of natural mud suspensions in the light of the new results reported above. An innovative feature of the present work is that we have inferred the constitutive equation of various mud samples in a simple shear flow directly from velocity profiles measured within the sample, with the help of nondestructive *magnetic resonance imaging* (MRI) technique with different rheometers. As typical mud suspensions we considered a bentonite-water mixture and the fine fraction of two debris flow materials.

## 2 EXPERIMENTAL TECHNIQUES AND PROCEDURES

When studying the rheology of complex fluids, it is difficult to determine whether a property exhibited by a material with a given rheometer reflects a true feature of the rheological behavior or is an experimental artifact. To reduce the risk of misinterpretation, it is important to perform rheometrical tests with different procedures and rheometers. A key point is that in classic rheometry the constitutive equation  $\tau = f(\dot{\gamma})$  (where  $\tau$  denotes the shear stress and  $\dot{\gamma}$  the shear rate) is inferred from the measurement of bulk quantities (e.g.,  $\Omega = g(C)$  where  $C$  is the torque and  $\Omega$  the rotation velocity for a rotational rheometer). For this procedure to be valid, a number of conditions must be met: the fluid must be homogeneous, belong to the class of incompressible simple fluids, that is, the stress tensor is a function of the strain rate tensor alone, etc. Since classic rheometers provide measurements of bulk quantities of the material only, the consistency of the conditions above cannot be tested. Thus, to avoid possible pitfalls in the interpretation of rheological properties of natural muds, it is useful to visualize the flow, as can be done, for example, with MRI techniques.

### 2.1 MRI rheometry

Magnetic resonance imaging can be combined with rheometry to determine flow characteristics and distribution of fluid density in viscometric flows (Callaghan 1999). When the resolution is sufficient, the data can be used to directly determine the constitutive equation of the fluid: the shear stress distribution is known from the momentum equation and can be associated with the strain rate distribution measured by MRI. For example, in a coaxial cylinder rheometer, when effects due to finite size,

normal stress difference, and fluid inertia are negligible, the shear stress is given as:

$$\tau = \frac{C}{2\pi hr^2} \quad (1)$$

where  $r$  is the distance from the central axis, and  $h$  the fluid height. In cylindrical coordinates, the shear rate is written:

$$\dot{\gamma} = r \frac{\partial(V/r)}{\partial r} \quad (2)$$

where  $V(r)$  is the tangential velocity. Eliminating  $r$  between (1) and (2) provides the relation between  $\tau$  and  $\dot{\gamma}$ , i.e., the constitutive equation of the fluid in a steady simple-shear flow.

Magnetic resonance imaging was performed with a Bruker set-up equipped with a vertical 0.5 T magnet fitted with shielded gradients, leaving a free bore of 25.5 cm and delivering a gradient of 50 mT/m with a rise time of 500 ms. The signal was collected within a linear birdcage coil 24 cm in length and 20 cm in diameter. More details on our technique, procedure, disturbing effects and validation can be found in the article by Raynaud et al. (2002). Here, successive velocity profiles were acquired in a short time period, ranging from 1 s to 30 s depending on the material. We thus observed possible transient effects and determine the velocity profile in steady state with a high signal-to-noise ratio by averaging the profiles over a more or less long time period after the transient stage.

The part of the rheometer inserted in the magnet was built in nonmagnetic materials. We used a coaxial cylinder geometry [inner cylinder:  $r_1 = 4$  cm (radius), length:  $h = 11.5$  cm; outer cylinder:  $r_2 = 6$  cm] and a cone and plate geometry (diameter: 13 cm, angle:  $8^\circ$ , truncature diameter: 3 cm). The surfaces of the Couette cylinder in contact with the fluid were covered with a sandpaper with an equivalent roughness of 200  $\mu\text{m}$ . This rheometer was remotely controlled by computer and it was possible to impose the velocity in step-by-step or continuous ramps. The regions imaged by NMR were as follows: for the Couette rheometer: a volume of 20 mm in the axial direction with a width (in the tangential direction) of 5 mm and a length of 70 mm. For the cone and plate rheometer: a cubic volume of 10-mm side-centered at a distance of 46 mm in the radial direction.

## 2.2 Inclined plane tests

One method for determining the apparent yield stress of fluids consists in determining the critical slope at which a uniform fluid layer starts to flow or the asymptotic thickness ( $h_0$ ) in the central region of a deposit of a finite volume of material simply poured over the inclined plane (Coussot et al. 1996). If slippage or other disturbing effects (sedimentation, surface tension, drying) can be neglected and if the thickness of the layer is much smaller than its longitudinal and lateral extent, the shear stress at the bottom is written:  $\tau_w = \rho g H \sin i$ , where  $g$  is gravity,  $i$  the inclination angle of the plane with respect to the horizontal,  $\rho$  the fluid density, and  $H$  the fluid thickness. At equilibrium ( $H = h_0$ ), the yield stress balances the wall shear stress so that the critical thickness (after stoppage) is related to the yield stress by:  $h_0 = \tau_c / (\rho g \sin i)$ .

For an ideal (nonthixotropic) yield stress fluid with no wall slip and for a fixed plane slope, as the fluid thickness decreases, the shear stress at the wall decreases so that the fluid velocity should continuously decrease over time (Coussot 1994). Conversely, if, after the mud volume has stopped over a plane with a fixed slope, the plane is further inclined, the fluid should start moving at a velocity that is a continuously increasing as a function of the difference in slope.

## 2.3 *Materials*

### 2.3.1 *Bentonite*

The bentonite suspensions were prepared from industrial grade Na-bentonite (Société française des bentonites et dérivés, France) mixed with tap water at different solid volume fractions (bentonite density:  $\rho = 2300 \text{ kg/m}^3$ ). Note that bentonite develops complex interactions with water, which in addition vary greatly with the electrolytes in the solution, but here we only focused on the reproducible mechanical trends of a given suspension of bentonite. The suspensions were first vigorously agitated continuously (with a mixer at 8000 rpm) for a period of about 10 min to ensure complete homogenization, and then left at rest for two days before the tests. This is a critical point because, apart from their thixotropic properties described below, these fluids tend to exhibit some long-term, irreversible aging that we could neglect here after this time of rest. Prior to the experiments, the suspension was strongly agitated by hand for 30 s and then stirred gently for 2 min. Immediately thereafter, it was poured into the outer cylinder; the rotating inner cylinder was immediately inserted at a velocity, which varied with the test. Sedimentation was always absent, even after several days at rest.

### 2.3.2 *Natural mud suspensions*

These materials were taken in the field. The first sample (mud A) comes from the Merdenson stream (Wallis, Switzerland) and mainly contains calc-schist sediment (illite, chlorite). The second field sample (mud B) was taken from the Illgraben stream (Wallis, Switzerland), which is one of the most active torrents in the Alps. The material is mainly made up of gypsum and sand dust (quartzite) and thus is poor in clays (illite). In both cases, the samples were collected a few days after the deposit of a debris flow, sieved (the upper sieve diameter was 0.4 mm), and dried. The dry material was remixed with tap water at a solid fraction of 48% for mud A and 65% for mud B. With these materials, sedimentation became apparent after about one hour at rest.

## 2.4 *Disturbing effects*

Various disturbing effects (inertia, relative motion of particles and liquid, free secondary flows, etc.) and the limitations of nuclear magnetic resonance (NMR) techniques for measuring velocity profiles of flowing suspensions have already been discussed in a recent paper to which the reader is referred (Raynaud et al. 2002).

## 3 EXPERIMENTAL RESULTS

### 3.1 *Bentonite*

We carried out MRI tests with the coaxial cylinders and the cone and plane in steady state, which, in those cases, was reached after approximately two minutes of preshear. Figure 1 reports the velocity profile across the gap for the coaxial cylinders while Fig. 2 shows the velocity profile for the cone and plane rheometer. For this case, we used the dimensionless height, i.e., the ratio of the absolute height to the mean height in the imaged volume (6.4 mm). A detailed combined MRI-Couette rheometry study of a more liquid bentonite suspension in steady and transient regimes is presented in the paper by Raynaud et al. (2002).

### 3.2 Natural muds

We performed MRI-coaxial cylinder tests at different velocities (Figs. 3–5). Contrary to bentonite suspensions, the steady state was not reached even after 1 hour of shear: the torque continuously decreased to almost half its initial value at an almost constant rate over this time period and the sheared region progressively decreased. In addition, the noise on the NMR signal was much more substantial than with bentonite suspensions, making it necessary to average the data over several minutes to obtain a relevant velocity profile. We compared the average velocity profile for the first 10 min and for the subsequent 10 min. Generally, these profiles were not significantly different (Figs. 3–5). Thus we can deduce that the velocity profile for a given test did not change significantly from the beginning to the end of acquisition during a 10-min test and our average profiles were a reliable representation of the velocity profile found in steady state before significant disturbance.

We also carried out inclined plane tests with natural muds. After preparation, the material was gently poured over an inclined plane so as to form a layer with a lateral and longitudinal extent larger than at least ten times its thickness. The flow was generally rapid in the first instants but each material eventually stopped much more rapidly than would an ideal yield stress fluid [in general several hours before surface tension effects became significant (Coussot 1994)]. Indeed the time for stoppage was of the order of 10 s for both natural muds. In addition, the stoppage of these materials on the plane was quite abrupt. When we plotted the total length of the deposit as a function of time (see Fig. 7), there was an apparent discontinuity in the slope of the experimental curve: the velocity suddenly dropped from a finite value to zero (Fig. 6). When, after stoppage of the materials, we increased the slope again, these materials did not start flowing again (even if we waited several minutes) before reaching a new critical slope,  $i_c$ , which was significantly larger than the initial one. This critical slope, and thus the corresponding pseudo-yield stress, increased with the rest time at the initial slope. In addition, flow generally started abruptly when  $i_c$  was reached. This behavior was reversible and reproducible: when the material was taken from the plane, mixed and poured again over the initial slope, a deposit shape similar to the initial one was obtained. Note that no slip occurred during these experiments: the

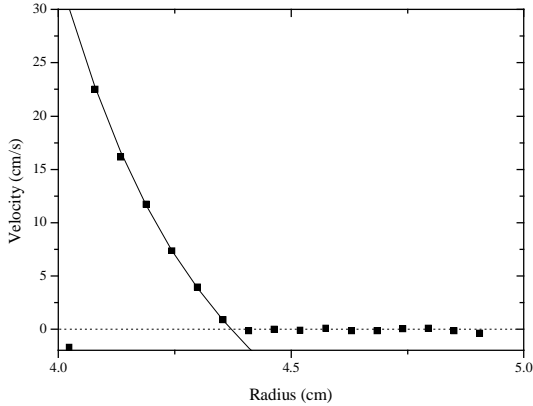


Figure 1: MRI velocity profile (velocity vs distance from the central axis) for the bentonite suspension in Couette geometry. Imposed rotation velocity: 80 rpm. The measured velocities in the sheared zone were fitted with a power-law expression (continuous line) in the form  $V = \alpha(R^{-(2-m)/m} - R)$  [deriving this expression leads to Eq. (4)], where the adjusted parameters are:  $r_c = 4.37$  cm ( $R = r/r_c$ ),  $\alpha = 15$  cm/s, and  $m = 0.142$ .

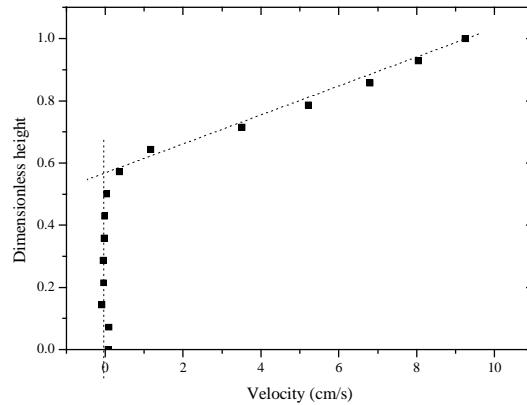


Figure 2: MRI velocity profile for the bentonite suspension in cone and plate geometry. Imposed rotation velocity: 20 rpm.

upper edge of the deposited fluid never moved during the entire series of tests. Similar observations have been reported for kaolin and bentonite suspensions (Coussot et al. 2002).

## 4 INTERPRETATION OF DATA AND DISCUSSION

### 4.1 *Instability on an inclined plane*

The abrupt stoppage on the initial slope and the abrupt start of the flow at a critical slope tend to demonstrate that there is some sort of instability below a critical velocity or shear rate. Indeed, for ideal yield stress fluids, the shear rate, and thus the mean velocity for a channelized flow, would progressively increase from zero, or decrease towards zero, as the applied stress is progressively increased above the yield stress, or decreased below the yield stress, respectively. Here the decrease or increase in velocity is abrupt. This instability is even clearer for long rest times: in this case we observed that the flow at the critical slope takes the form of an initial fracture along a surface (with a horseshoe shape as viewed from above, which can be observed in certain landslides) followed by a “liquefaction” (here taking the form of a rapid transition from a rigid to a flowing material) as the material moves downwards and accelerates. These different effects contrast with those expected for an ideal yield stress fluid. It follows that there is a need to explore the rheological behavior of these suspensions in greater detail and in particular the relationship between the steady state flow characteristics, the flow instability under some conditions, and the thixotropic behavior of the material.

### 4.2 *Coexistence of fluid and solid behavior within flowing suspensions*

Let us consider the velocity profiles obtained under different conditions using the MRI-Couette rheometer (Figs. 1–5). Velocity profiles are typically made of two clearly distinct parts:

1. Close to the inner cylinder the slope of the profile remains larger than a finite value, i.e., when it is more than several millimeters, the velocity approximately follows a straight, inclined line,

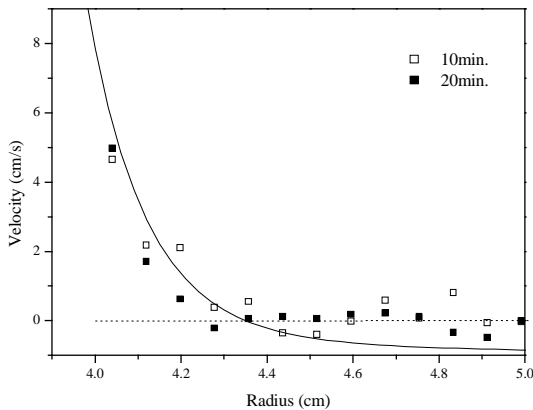


Figure 3: MRI velocity profile (velocity vs distance from the central axis) for the mud suspension A in Couette geometry. Imposed rotation velocity: 20 rpm. The measured velocities in the sheared zone were fitted with a power-law expression (continuous line) in the form  $V = \alpha(R^{-(2-m)/m} - R)$ , where the adjusted parameters are:  $r_c = 4.3$  cm ( $R = r/r_c$ ),  $\alpha = 15$  cm/s, and  $m = 0.142$ .

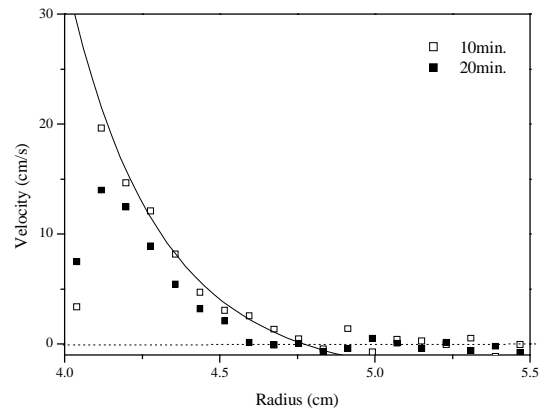


Figure 4: MRI velocity profile (velocity vs distance from the central axis) for the mud suspension A in Couette geometry. Imposed rotation velocity: 80 rpm. The measured velocities in the sheared zone were fitted with a power-law expression (continuous line) in the form  $V = \alpha(R^{-(2-m)/m} - R)$ , where the adjusted parameters are:  $r_c = 4.77$  cm ( $R = r/r_c$ ),  $\alpha = 3.1$  cm/s, and  $m = 0.133$ .

which eventually intersects the abscissa axis at a critical radius  $r_c$ .

2. Elsewhere the velocity is close to zero and, although it fluctuates, it remains smaller than the uncertainty on measurements.

These two regions can thus be described as a region flowing at a rate larger than  $\dot{\gamma}_c$  and a region without flow ( $\dot{\gamma} = 0$  for  $r \geq r_c$ ). In some cases, when  $\dot{\gamma}_c$  is not large at our typical scale of observation, the discontinuity may be harder to observe. The existence of this discontinuity can nevertheless be proved because various curves (for example, associated with exponential or power-law equations) may be fitted to experimental data while a flat curve is used for describing the velocity profile in the unsheared zone. The slope discontinuity clearly appears at the intersection between the two curves (Figs. 1–5). It is worth noting that there might be some very slow motion in the supposed rigid region but here we only emphasize the coexistence of two regimes with two very different behavior types. Here it appears that in steady state, within the uncertainty of our measurements, the fluid is either flowing at a significant rate or not sheared at all, depending on the relative values of the applied stress and a critical stress, here associated to  $r_c$ .

Such profiles are fundamentally different from those expected for fluids whose behavior is well described by the usual yield stress models: these models predict a continuous transition from the sheared to the unsheared region, i.e., the slope of the velocity profile progressively tends towards zero close to  $r_c$ . The velocity profiles associated with any type of model for ideal yield stress fluids, such as the Bingham or Herschel-Bulkley models, cannot be fitted satisfactorily to these data over the whole range of radii. A region of almost constant shear rate is not consistent with these models, in particular for stresses close to the yield stress. For example, a Bingham model may be fitted to the data over a significant range of radii close to the inner cylinder, but there necessarily remains a region of complete discrepancy near the outer cylinder.

Such behavior implies some peculiar effect at low velocities: the fluid cannot *a priori* be sheared homogeneously at a small rate, so that when a low relative velocity is imposed, one expects some sort of shear-banding effect. This is what we observed in cone and plane tests for the bentonite: the fluid

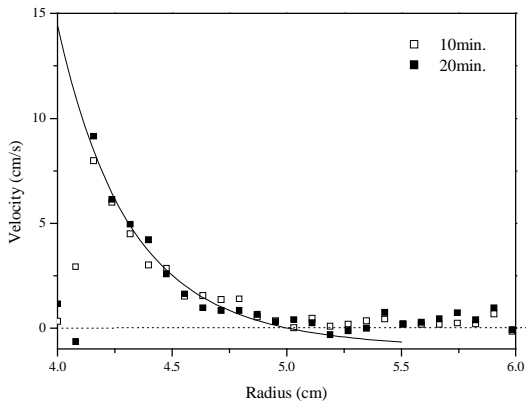


Figure 5: MRI velocity profile (velocity vs distance from the central axis) for the mud suspension B in Couette geometry. Imposed rotation velocity: 35 rpm. The measured velocities in the sheared zone were fitted with a power-law expression (continuous line) in the form  $V = \alpha(R^{-(2-m)/m} - R)$ , where the adjusted parameters are:  $r_c = 5$  cm ( $R = r/r_c$ ),  $\alpha = 0.83$  cm/s, and  $m = 0.333$ .

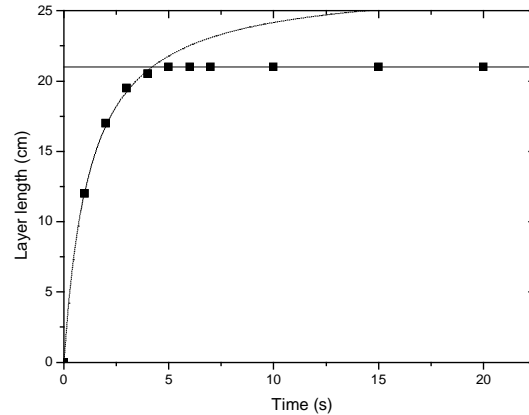


Figure 6: Flow of a mud poured over an inclined plane: length of the mud layer as a function of time. The thin dotted line is a “spline” function fitted to the data before reaching the length (continuous line) corresponding to complete stoppage.

was separated into a region of rapid shear at a roughly constant rate and a region of no shear at all. In fact this velocity profile results from the concentration of shear in the regions of higher stresses, i.e., where the horizontal fluid surface is slightly smaller because of a small deformation of the peripheral free surface. Even with a very low angle cone and plate geometry, the peripheral free surface is never perfect and such regions exist. Since by definition  $V(r_c) = 0$ , it results from (2) that the critical shear rate, below which no flow homogeneous flow can occur, is simply related to the slope of the velocity profile in Couette flows

$$\dot{\gamma}_c = \left( \frac{dV}{dr} \right)_{r_c} \quad (3)$$

For the bentonite suspension, we find  $\dot{\gamma} = 42 \text{ s}^{-1}$  from the Couette flow and  $\dot{\gamma}_c \approx 35 \text{ s}^{-1}$  from the cone and plate flow. In this case the critical shear rate is simply found from the ratio of the maximum velocity to the sheared thickness. The qualitative consistency of our different results and of the corresponding analysis thus becomes apparent.

#### 4.3 Behavior in the sheared region

The Herschel-Bulkley model is not the best candidate to fairly describe the rheological properties of our mud suspensions for at least two reasons: (i) it cannot describe the instability observed with the inclined channel when the mud sample is set in motion by tilting the channel, (ii) the observed shear-rate discontinuity at the interface between the sheared and unsheared regions is not consistent with the Herschel-Bulkley model predictions. Facing a similar problem with bentonite dispersions, Raynaud et al. (2002) suggested using a piecewise rheological model, which assumes that yielding results from a shear localization instead of an excess of stress. For simple shear flows in a steady state, the flow condition in the Raynaud et al.'s model is given by:  $\dot{\gamma} > \dot{\gamma}_c(\tau_0)$  whereas in the Herschel-Bulkley it is described by:  $\tau > \tau_0$ . For the sheared region, Raynaud et al. suggested that the shear stress is related to the shear rate by a power-law relationship:

$$\tau = A\dot{\gamma}^m \quad (4)$$

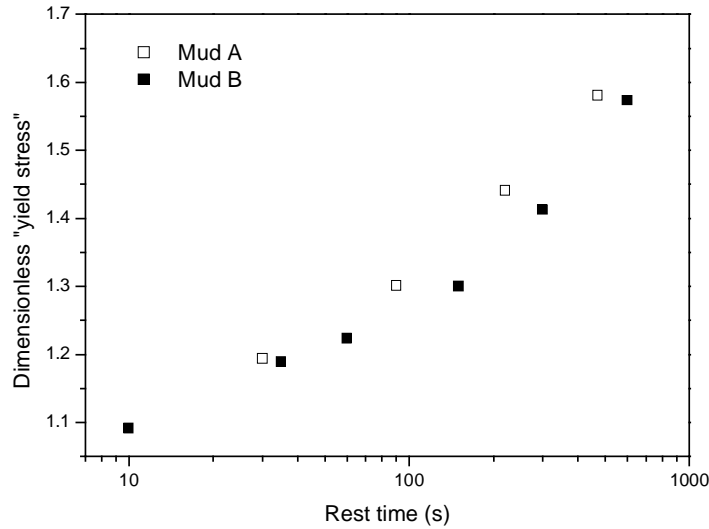


Figure 7: Dimensionless yield stress, i.e., ratio of the stress associated to the critical slope for flow start to that associated to flow stoppage at the initial slope, as a function of the time of rest at the initial slope. The thickness of the fluid layer at stoppage was: (A) 2.1 cm; (B) 2.5 cm, so that the yield stress was: (A) 93 Pa; (B) 143 Pa.



with  $A = \tau_0 (mr_c/(2\alpha))^m$ ,  $m$  and  $\alpha$  being two parameters to be fitted. This expression differs substantially from the Herschel-Bulkley model, which states that:  $\tau = \tau_0 + \beta\dot{\gamma}^p$ , where  $p$  and  $\beta$  being two adjustable parameters. Note that in both cases, there is a dependence of the shear stress on the yield stress  $\tau_0$  but this dependence occurs as an additional contribution in the Herschel-Bulkley model whereas it appears in the coefficient  $A$  for the model proposed by Raynaud et al. In both models, the stress state in the unsheared zone is not undetermined and usually can be computed by solving the static equilibrium equations. Note that, since the Herschel-Bulkley model obeys a plastic rule, the state stress must be included inside the yield surface while such a constraint is absent in the model proposed by Raynaud et al.

#### 4.4 *Transient behavior*

The flow instability below a critical shear rate is necessarily associated with some thixotropic effects. This has been in particular shown with bentonite suspensions (Coussot et al. 2002): the velocity profile after a sudden change in imposed velocity takes some time to reach its steady state form and during this transient stage it changes progressively and significantly. No such effect could be observed with natural muds because of the relatively long duration necessary for data acquisition. Nevertheless with natural muds an additional effect occurred, which has nothing to do with a transient behavior of a homogeneous fluid. This is a segregation effect. This phenomenon was observed from:

1. A difference in the NMR (proton density) signal distribution along a radial portion before and after shear; because the signal intensity depends on various characteristics of the liquid fraction in the material it remains difficult and uncertain to analyze it relevantly; however the observed difference suggests a change in the distribution of liquid density.
2. The continuous and almost constant decrease in torque over a long period of time, which in general does not simply reflect a thixotropic effect.
3. The continuous displacement of the velocity profile towards the inner cylinder, with no apparent asymptotic value, also in contradiction with observations with thixotropic materials.
4. The apparent difference (from rough sampling) in the solid fraction of the suspension close to the outer cylinder and cup bottom, and close to the inner cylinder, after shear.

Such effects did not occur with the clay suspensions because of the absence of particles of a size larger than 0.1 mm. The question of their effective quantitative role on the apparent behavior remains open. Anyway, a relevant study of the constitutive equation of natural mud suspensions or debris flows cannot ignore segregation, phenomenon which appears to be an integral part of clay and natural mud suspension behavior during flows.

## 5 CONCLUSIONS AND PERSPECTIVES

Since Johnson (1970) and Johnson Rodine (1984), it has been fully recognized that natural gravity-driven flows involving a mixture of mud and debris exhibit viscoplastic properties. So far Bingham or Herschel-Bulkley models have been most often used as constitutive equations of the bulk material mobilized by these flows. The present accurate measurements have demonstrated that the true behavior of (interstitial) mud is much more complex than predicted by usual viscoplastic models. There are some crucial differences between the behavior predicted by a Herschel-Bulkley model and the behavior observed experimentally by using MRI techniques that are useful to review here.

For the sake of simplicity, we will focus our attention on simple shear flows. In the Herschel-Bulkley model, sustained deformation is possible within the material provided that the shear stress exceeds a critical value, identified as the yield stress. The yield stress is found to be a function of the solid concentration in particles (Ancey & Jorrot 2001). In our experiments on natural muds, we have also found that the transition from rest to motion can be described by using a condition on a critical stress, but this quantity, although intrinsic to the material, depends on the rest time of the material. The dependence of the yield stress on the time of rest has two important implications from the rheological viewpoint. First, since this dependence is strongly marked, a further equation (a kind of kinetic equation for the variation of yield stress with time) is needed (Coussot et al. 2002). Second, the value of the yield stress depends on the procedure used for determining it. From a phenomenological point of view, the consequences of the time-dependent properties of the yield stress on bulk behavior of mudflows are unclear. At the least, the rapid increase in yield stress with rest time implies a significant consolidation of mud deposits: much more energy is required for muddy materials to start flowing again after stoppage than to go on flowing. In short, we have found:

1. With the natural muds, the MRI data seemed to be much affected by signal noise. There nevertheless clearly appeared a sheared and an unsheared zones.
2. Two phenomenological constitutive equations, the Herschel-Bulkley and an alternative expression proposed by Raynaud et al. (2002), could be fitted in such a limited range of shear rates and with such an uncertainty on data.
3. The critical point which leads us to consider that the behavior natural muds is better described by Raynaud et al.'s equation is the instability of flows over an inclined plane. This instability is similar to that observed with bentonite suspensions and is a direct consequence of the incapacity of the fluid to flow steadily when the shear rate drops below a critical value. This instability is also consistent with the slope rupture in the velocity profile determined by MRI.
4. It is worth noting that, in fact, the model by Raynaud et al.'s (2002) is nothing but a means to express the behavior type leading to a slope rupture in the velocity profile, or more generally the instability associated to a critical shear rate. At this stage, we cannot pretend that this model represents the general behavior of natural muds over a wide range of shear rate.

## ACKNOWLEDGMENTS

We thank PNRN (Programme National sur les Risques Naturels) for its support of this research, J.C. Baudez (Cemagref), F. Bertrand, P. Moucheront and J.P. Guilbaud (LMSGC) for their technical support, O. Coussy for helpful comments and Eric Bardou (Ecole Polytechnique Fédérale de Lausanne) for providing samples of debris flows.

## REFERENCES

- Alderman, N.J., Meeten, G.H. & Sherwood, J.D. 1991. Vane rheometry of bentonite gels. *Journal of Non-Newtonian Fluid Mechanics* 39: 291–310.
- Ancey, C. & Jorrot, H. 2001. Yield stress for particle suspensions within a clay dispersion. *Journal of Rheology* 45: 297–319.
- Callaghan, P.T. 1999. Rheo-NMR: nuclear magnetic resonance and the rheology of complex fluids. *Reports in Progress of Physics* 62: 599–670.

- Cheng, D.C-H. 1986. Yield stress: a time-dependent property and how to measure it. *Rheologica Acta* 25: 542–554.
- Contreras, S.M. & Davies, T.R.H. 2000. Coarse-grained debris-flows: hysteresis and time-dependent rheology. *Journal of Hydraulic Engineering* 126: 938–941.
- Coussot, P. 1994. Steady, laminar flow of concentrated suspensions in open channel. *Journal of Hydraulic Research* 32: 535–559.
- Coussot, P. 1997. *Mudflow Rheology and Dynamics*. IAHR Monograph Series. Rotterdam: Balkema.
- Coussot, P., Leonov, A.I. & Piau, J.M. 1993. Rheology of concentrated dispersed systems in low molecular weight matrix. *Journal of Non-Newtonian Fluid Mechanics* 46: 179–217.
- Coussot, P., Proust, S. & Ancey, C. 1996. Rheological interpretation of deposits of yield stress fluids. *Journal of Non-Newtonian Fluid Mechanics*, 66: 55–70.
- Coussot, P., Nguyen, D.Q., Huynh, H.T. & Bonn, D. 2002. Viscosity bifurcation in thixotropic, yielding fluids. *Journal of Rheology* 46: 573–589.
- Johnson, A.M. 1970. *Physical Processes in Geology*. San Francisco: Freeman, Cooper & Co.
- Johnson, A.M. & Martosudarmo, S.Y. 1997. Discrimination between inertial and macro-viscous flows of fine-grained debris with a rolling-sleeve rheometer. In C.L. Chen (ed.), *Debris-Flow Hazards: Mechanics, Prediction, and Assessment; Proceedings 1st International DFHM Conference, San Francisco, CA, USA, August 7-9, 1997*: 229–238. New York: ASCE.
- Johnson, A.M., & Rodine, J.R. 1984. Debris flow. In D. Brunsten & D.B. Prior (eds), *Slope Instability*, pp. 257–362. New York: John Wiley & Sons.
- Major, J.J. & Pierson, T.C. 1992. Debris flow rheology: experimental analysis of fine-grained slurries. *Water Resources Research* 28: 841–857.
- Nguyen, Q.D. & Boger, D.V. 1992. Measuring the flow properties of yield stress fluids. *Annual Review of Fluid Mechanics* 24: 47–88.
- O'Brien, J.S. & Julien, P.Y. 1988. Laboratory analysis of mudflow properties. *Journal Hydraulic Engineering* 114: 877–887.
- Piau, J.-M. 1979. Non-Newtonian fluids. In *Techniques de l'Ingénieur*: vol. A710, 1–16, vol. A711, 1–24. Paris: Istral. (In French).
- Pignon, F., Magnin, A. & Piau, J.-M.. 1996. Thixotropic colloidal suspensions and flow curves with minimum: identification of flow regimes and rheometric consequences. *Journal of Rheology* 40: 573–587.
- Raynaud, J.S., Moucheron P. , Baudez, J.C., Bertrand, F. , Guilbaud, J.P. & Coussot, P. 2002. Direct determination by NMR of the thixotropic and yielding behavior of suspensions. *Journal of Rheology*. 46: 709–732.
- Wildemuth, C.R. & Williams, M.C. 1985. A new interpretation of viscosity and yield stress in dense slurries: coal and other irregular particles. *Rheologica Acta* 24: 75–91